

Technical report 14-011

An analytic model for a ^{13}C isotope separation process by cryogenic distillation*

D.C. Dumitrache, I. Inoan, and B. De Schutter

If you want to cite this report, please use the following reference instead:

D.C. Dumitrache, I. Inoan, and B. De Schutter, “An analytic model for a ^{13}C isotope separation process by cryogenic distillation,” *Journal of Process Control*, vol. 24, no. 5, pp. 463–474, May 2014.

Delft Center for Systems and Control
Delft University of Technology
Mekelweg 2, 2628 CD Delft
The Netherlands
phone: +31-15-278.24.73 (secretary)
URL: <https://www.dsc.tudelft.nl>

*This report can also be downloaded via https://pub.deschutter.info/abs/14_011.html

An analytic model for a ^{13}C isotope separation process by cryogenic distillation

Dan Călin Dumitrache^{a,*}, Iulia Inoan^a, Bart De Schutter^b

^a*Department of Automation, Technical University of Cluj-Napoca, Memorandumului 28, 400114, Cluj-Napoca, Romania*

^b*Delft Center for Systems and Control, Delft University of Technology, Mekelweg 2, 2628 CD Delft, The Netherlands*

Abstract

In this paper we present a structured approach to the modeling of an isotope separation plant that makes use of distillation principles for ^{13}C isotope separation. In the first part of the paper, after a brief review of isotope separation processes with an accent on isotope separation by distillation, we define our initial-boundary-value problem, which is a partial differential equation. By applying the Laplace transform to the partial differential equation that governs the evolution of the desired isotope with respect to height and time, we obtain a linear homogeneous ordinary differential equation. After solving the obtained ordinary differential equation, we use Heaviside's expansion theorem to find the inverse Laplace transform, and thus, the analytic model of the isotope separation process follows. Using the analytic model it is possible to determine the concentration of the desired isotope at any height, at any moment of time, with respect to plant parameters and thus, expensive experiments can be avoided. In the second part of the paper we use the analytic model to simulate the isotope separation process, followed by the assessment of the results against experimental data.

Keywords: Mathematical modeling, Isotope separation, Cryogenic distillation, Analytic model, Simulation

1. Introduction

Isotope-based applications are met in a variety of fields such as chemistry, medicine, hydrology, and energy. The use of isotopic labeled compounds in order to explore different chemical, biological, or hydrological mechanisms is well known [1–4]. Likewise, the practical applications of radioisotopes in energy generation has been studied extensively, at this moment resulting in 436 working nuclear plants worldwide and another 63 plants under construction [5–8]. Moreover, there is an increasing interest in the use of isotopes in medical investigations [9, 10]. Particularly,

*Corresponding author. Tel.: +40 740 365 167; Fax: +40 266 313 058;
Preprint submitted to Elsevier
E-mail address: dan.dumitrache@aut.utcluj.ro

the ^{13}C isotope plays an important role in oceanic and atmospheric studies, as well as in medical diagnosis based on breath CO_2 tests ($^{13}\text{C}/^{12}\text{C}$ ratio) used to avoid common invasive procedures [11, 12].

In order to increase the concentration of a certain isotope, one can adopt an isotope separation method. Isotope separation techniques depend on several factors, among which are the properties of the chemical compound involved, the various applications that require different concentrations, and the cost of the isotope separation process [13–17].

Urey [18] was among the first to show that the isotopic compounds do not only differ in thermodynamical properties but also in their physical and chemical properties. In [19] Bigeleisen and Mayer proposed a calculation method for the equilibrium constant of the isotopic exchange reactions. Bigeleisen continued his work on isotopes providing a comprehensive review in [13] and a survey with emphasis on isotope effects in [15]. A description of various isotope separation techniques can be found in [4, 20–22]. Cohen has developed the general theory of multistage isotope separation processes in [23], also treating briefly the behavior of liquid-gas countercurrent chemical exchange towers. In [24] London provides an insightful study on isotope separation. Referring to ^{13}C isotope separation processes, McInteer presents in [25] the design issues of a ^{13}C cryogenic rectification plant, while Andreev et al. [26] present the characteristics of different ^{13}C isotope separation plants. In [27], following first-principles knowledge, we have presented a structured modeling approach for a ^{13}C isotope separation process that uses distillation principles. We acknowledge the work of Zemansky [28] regarding thermal phenomena, while in the field of mass transfer and separation processes Cussler, King, and Benitez [29–31] are insightful references. Concerning the dynamics and control of distillation columns, Skogestad et al. [32–36] provide a detailed and comprehensible treatment. Regarding distributed parameter systems and partial differential equations we mention [37–41]. In the field of complex analysis and its applications we acknowledge the work of Townsend, LePage, Duffy, and Brown [42–45], while in the field of numerical analysis [46–48] represent standard works.

Isotope separation processes have, like most physical, chemical, or biological processes, a coupled time-space nature, and thus they belong to the class of distributed parameter systems [37, 38, 49, 50]. Modeling of a distributed parameter system, in general, and modeling of an isotope separation process in particular, is a time-consuming task and requires knowledge from different fields. Numerical methods are widely used in order to solve different mathematical models. However, closed-form solutions (i.e. analytical solutions) are preferred, since they are in general faster and allow a more meaningful analysis of the process and they ease the linking to

the physics of the process [40, 51–54].

The objective of this paper is to provide the analytic solution of the model of a ^{13}C isotope separation process followed by the simulation of the isotope separation plant and hence, to provide a basis for future studies in optimization and process control design. The main contribution of this study consists in the comprehensive determination of the analytic model of the ^{13}C isotope separation process by cryogenic distillation of carbon monoxide. This approach is applicable to other isotope separation processes as well. The assessment of the analytic model is made via simulation. Using the analytic model one can determine the concentration of desired isotope at any height and at any moment of time, with respect to plant parameters and thus, expensive experiments can be avoided. To the authors' best knowledge we are the first to treat these issues for a ^{13}C cryogenic distillation plant.

The paper is structured as follows. In Section 2 we give a brief account of isotope separation processes with emphasis on isotope separation by distillation, followed by a short review of the experimental pilot-scale plant developed at the National Institute for Research and Development of Isotopic and Molecular Technologies in Cluj-Napoca, Romania. In Section 3, based on the linear partial differential equation that governs the evolution of the desired isotope concentration with respect to space and time, we derive the analytic model of the isotope separation process. In Section 4 we use the obtained analytic model to determine the evolution of the concentration of the desired isotopic compound at both ends of the distillation column. The concentration evolution is compared with experimental data. Next, we simulate the isotope concentration distribution in the column followed by the assessment of the results. Section 5 concludes the paper.

The list of tables and figures present the tables and figures referred to within this paper. The most frequent notations used in this paper are listed in Table 1.

List of Tables

| | | |
|---|--|----|
| 1 | Nomenclature | 5 |
| 2 | Parameters of the analytical solution and the heights of the rectifying and stripping section in the case of all three isotope separation experiments. | 23 |
| 3 | The values of $(\gamma(s_j)Z_r)$ and $(\gamma(\tilde{s}_j)Z_s)$ when $j = 2, 3, 4, 5$, and 6 in the case of all three isotope separation experiments. | 23 |
| 4 | The values of the maximum and average relative error between simulated and measured data at the ends of the separation column. | 27 |

83 List of Figures

| | | | |
|----|---|---|----|
| 84 | 1 | Experimental pilot-scale cryogenic distillation plant with condenser K, distillation | |
| 85 | | column C, reboiler B, vacuum jacket VJ, rough pump RP, diffusion pump DP, | |
| 86 | | temperature sensors T_1 – T_2 , manometers M_1 – M_3 , level sensor L, feed reservoir | |
| 87 | | FR, buffer tank BT, and waste reservoir WR. | 7 |
| 88 | 2 | Schematic representation of the ^{13}C cryogenic distillation and of the column's | |
| 89 | | rectifying and stripping section. | 9 |
| 90 | 3 | Graphical representation of the functions $y_1(\gamma(s)Z_r)$, $y_1(\gamma(\tilde{s})Z_s)$ and $y_2(\gamma(s)Z_r)$, | |
| 91 | | $y_2(\gamma(\tilde{s})Z_s)$ | 18 |
| 92 | 4 | ^{13}C concentration evolution according to the analytical solution and ^{13}C concen- | |
| 93 | | trations achieved by the pilot-scale experimental plant. | 24 |
| 94 | 5 | Relative errors between simulated and measured data at the end of the rectifying | |
| 95 | | section (bottom of the column) and at the end of the stripping section (top of the | |
| 96 | | column). | 25 |
| 97 | 6 | ^{13}C isotope concentration distribution with respect to time and height. | 26 |

98 2. Isotope separation process

99 Isotope separation techniques have their origins in the isotope effects of different isotopic
100 compounds that arise from the differences in the nuclear properties of the isotopes. Some prac-
101 tical isotope separation methods are based on chemical exchange processes, gaseous diffusion,
102 gas centrifuge, laser separation, electromagnetic isotope separation (which is a form of mass
103 spectrometry), and distillation [21, 22].

104 2.1. Isotope separation by cryogenic distillation

105 In the case of light elements like boron, carbon, nitrogen, or oxygen, due to the large relative
106 mass difference, distillation was successfully applied to the separation of isotopes [17, 24]. Separa-
107 tion processes by distillation are based on the notion of *relative volatility*, which is a comparative
108 measure for the vapor pressure of the components within a mixture [30, 32].

109 Regarding the separation of carbon isotopes, it has been shown that the vapor pressure
110 isotope effect is the highest in the case of carbon monoxide (CO) and methane (CH_4). Thus,
111 these substances are preferred as raw material in ^{13}C isotope separation by distillation. Since
112 both carbon monoxide and methane are gaseous in standard conditions, cryogenic distillation is
113 applied [26, 55, 56].

Table 1: Nomenclature

| <i>Latin symbols</i> | | |
|----------------------|--|------------------------|
| F | feed flow rate | mol/(m ² s) |
| H | hold-up per unit volume | mol/m ³ |
| K | volumetric overall mass transfer coefficient | mol/(m ³ s) |
| L | liquid molar flow rate per unit area | mol/(m ² s) |
| n | ¹³ CO mole fraction in vapor phase | — |
| N | ¹³ CO mole fraction in liquid phase | — |
| P | product flow rate | mol/(m ² s) |
| t | time | s |
| V | vapor molar flow rate per unit area | mol/(m ² s) |
| W | waste flow rate | mol/(m ² s) |
| z | height (position) | m |
| Z | total height | m |
| <i>Greek symbols</i> | | |
| α | relative volatility | — |
| ε | enrichment factor | — |
| τ | molar transfer rate per unit volume | mol/(m ³ s) |
| <i>Superscript</i> | | |
| 0 | pure component | — |
| 13 | atomic number | — |
| <i>Subscript</i> | | |
| 0 | natural abundance | — |
| ¹³ CO | isotopic species | — |
| c | column | — |
| F | is referring to feed flow rate | — |
| g | general | — |
| j | index | — |
| k | index | — |
| l | liquid | — |
| p | particular | — |
| P | is referring to product flow rate | — |
| r | rectifying | — |
| s | stripping | — |
| v | vapor | — |
| W | is referring to waste flow rate | — |

Since this paper treats the modeling and simulation of a ^{13}C separation plant by cryogenic distillation of carbon monoxide, in the following we will refer to carbon monoxide. Due to the fact that carbon has two stable isotopes, ^{12}C and ^{13}C with a natural abundance of 98.89% and 1.11% respectively, and oxygen has three stable isotope, ^{16}O , ^{17}O , and ^{18}O with natural abundances of 99.76%, 0.04%, and 0.20% respectively, in the process of cryogenic distillation of carbon monoxide, six molecular species are involved. However, considering the low natural abundances of ^{17}O and ^{18}O , it is reasonable to relate the carbon monoxide to a binary mixture form of $^{12}\text{C}^{16}\text{O}$ and $^{13}\text{C}^{16}\text{O}$ [25]. The separation factor, when the ^{13}CO (i.e. the less volatile component) is the product, is expressed by¹ [32]:

$$\alpha = \frac{p_{^{12}\text{CO}}^0}{p_{^{13}\text{CO}}^0} = \frac{N/(1-N)}{n/(1-n)} \quad (1)$$

where $p_{^{12}\text{CO}}^0$ and $p_{^{13}\text{CO}}^0$ are the vapor pressure of the pure components ^{12}CO and ^{13}CO , N and n refer to the ^{13}CO mole fraction in the liquid phase respectively vapor phase, while $1-N$ and $1-n$ are the ^{12}CO mole fraction in the liquid and vapor phase, respectively.

An accepted value for α , at the boiling point of CO in normal conditions (i.e. 81.6 K), is $\alpha = 1.0069$ [26, 57].

2.2. The pilot-scale experimental plant

At the National Institute for Research and Development of Isotopic and Molecular Technologies, Cluj-Napoca, Romania, an experimental ^{13}C isotope separation plant has been developed. The plant is shown in Fig. 1. The configuration consists of a single column of 7000 mm in height with an inner diameter of 16 mm, packed with Heli-Pak stainless steel wire of 1.8 mm×1.8 mm×0.2 mm.

The experiments used to validate the analytical solution were conducted in total-reflux regime at a pressure of approximately 0.8×10^5 Pa.

The distillation column is fed with highly purified carbon monoxide in liquid state. From the top of the column the waste gas (^{12}CO enriched) is withdrawn, while from the bottom of the column the product (^{13}CO enriched) is taken out. A variable heating resistance (up to 150 W) ensures the vapor stream, while the total condenser provides the reflux. The total condenser uses liquid nitrogen as cooling agent (N_2 has a boiling point in normal conditions of 77.3 K [57]).

¹For brevity, in the following, the atomic number of the oxygen is omitted, i.e. we use ^{13}CO as a short notation for $^{13}\text{C}^{16}\text{O}$. Similarly, $^{12}\text{C}^{16}\text{O}$ is indicated as ^{12}CO .

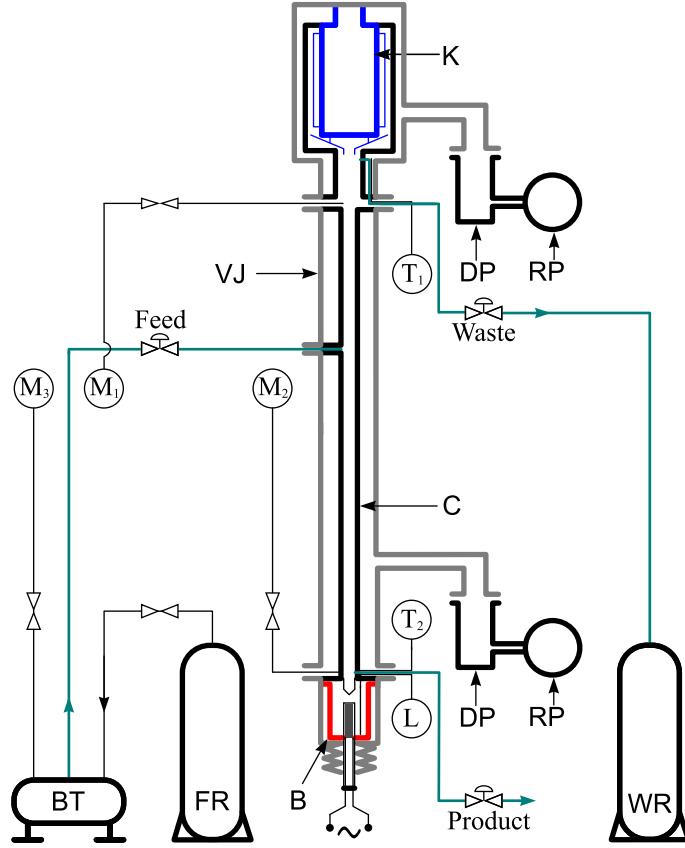


Figure 1: Experimental pilot-scale cryogenic distillation plant with condenser K, distillation column C, reboiler B, vacuum jacket VJ, rough pump RP, diffusion pump DP, temperature sensors T_1 – T_2 , manometers M_1 – M_3 , level sensor L, feed reservoir FR, buffer tank BT, and waste reservoir WR.

141 A multilayered vacuum jacket provides the thermal insulation. The pressure within the jacket
 142 was 1.07×10^{-2} Pa [27].

143 2.3. Isotope separation PDE model

144 In a previous paper [27], we have derived, using first-principles knowledge, a full nonlinear
 145 model for the isotope separation by cryogenic distillation. Due to the complexity of the full
 146 nonlinear model we have considered two alternative modeling approaches. Two simplified models
 147 followed, a quasi-linear model and, when the isotope concentration achieved by the separation
 148 plant was low, a linear model. Subsequently, we have shown that the linear model is a valid
 149 modeling approach for ^{13}C isotope separation by cryogenic distillation.

150 The linear model for the isotope separation process in a rectifying column is described by the

151 following partial differential equation (PDE):

$$(H_l + H_v) \frac{\partial N}{\partial t} = \left(\frac{LV}{K} \right) \frac{\partial^2 N}{\partial z^2} - [P + L(\alpha - 1)] \frac{\partial N}{\partial z} \quad (2)$$

152 where $H_l + H_v$ is the total hold-up per unit volume of the raw material in the column, both
 153 in liquid and vapor phase, L and V stand for the liquid and vapor molar flow rates per unit
 154 area, K is the volumetric overall mass transfer coefficient, while P is the product flow rate given
 155 by² $P = L - V$. The initial condition is represented by the natural abundance of ^{13}C , while
 156 the boundary conditions are determined by the concentration achieved at the top of the column
 157 ($z = 0$) respectively at the bottom of the column ($z = Z_c$) [27]. In the following, based on the
 158 above isotope separation PDE model, we will determine the analytical solution of the isotope
 159 separation process.

160 3. Analytical solution of the model of the isotope separation process

161 It is well known that the Laplace transform is a powerful tool for transforming initial-value
 162 problems involving ordinary differential equations (ODE) into algebraic equations [58, 59]. The
 163 Laplace transform can be also applied for transforming a PDE into another PDE with one
 164 independent variable less, or, if the original PDE had two independent variables, into an ODE
 165 [60, 61]. In this section, based on the PDE model that governs the evolution of the desired isotope
 166 during the isotope separation process, we will define our initial-boundary-value problem. Using
 167 the Laplace transform we will obtain a linear homogeneous ODE. After solving the obtained
 168 ODE, by applying the inverse Laplace transform we will obtain the analytical solution of the
 169 model of the isotope separation process.

170 Fig. 2(a) shows the schematic representation of the ^{13}C cryogenic distillation plant. The
 171 plant operates in extraction regime. We have denoted by F the feed flow rate, by P the product
 172 flow rate, and by W the waste flow rate. The feed point divides the column in two sections,
 173 the rectifying section and the stripping section. When the product is represented by the less
 174 volatile component, the rectifying section starts from the feeding point and ends at the bottom
 175 of the column, while the stripping section starts from the feeding point and ends at the top of
 176 the column³. In steady state, from the end of the rectifying section of the column, the product is

²When the product is represented by the less volatile component.

³When the product is represented by the more volatile component, the rectifying section starts from the feeding point and ends at the top of the column, while the stripping section starts from the feeding point and ends at the bottom of the column.

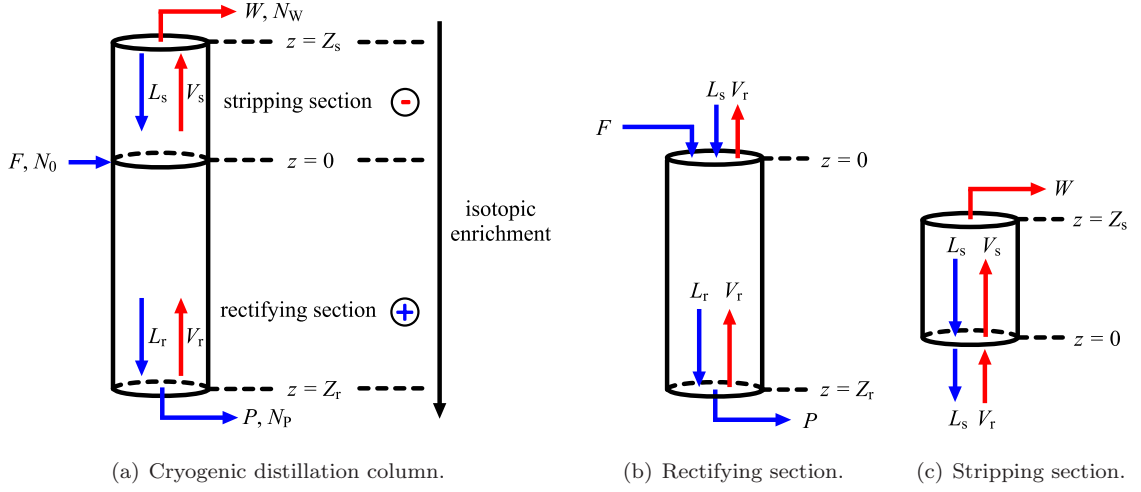


Figure 2: Schematic representation of the ^{13}C cryogenic distillation and of the column's rectifying and stripping section.

177 taken out with a constant flow rate P and a ^{13}C concentration equal to N_p . From the end of the
 178 stripping section of the column, the waste is taken out with a constant flow rate W and a ^{13}C
 179 concentration equal to N_w . Highly purified carbon monoxide is fed the column with a constant
 180 flow rate F and a ^{13}C concentration equal to the ^{13}C natural abundance, N_0 . The internal liquid
 181 and vapor molar flow rates per unit area in the rectifying section are denoted by L_r and V_r and
 182 by L_s and V_s in the stripping section.

183 In the rectifying section, the gradient of the height is positive by convention, while in the
 184 stripping section it is negative [13, 15, 23, 24]. The feeding point corresponds to height $z = 0$.
 185 The bottom of the column corresponds to the height $z = Z_r$ ($Z_r > 0$) and the top of the column
 186 to the height $z = Z_s$ ($Z_s < 0$).

187 In the following we will derive the analytical solution of the isotope separation process in the
 188 rectifying section of the ^{13}C cryogenic distillation column. The obtained model is applicable to
 189 the stripping section too; however, in that case, the height gradient will be negative.

190 3.1. Defining the initial-boundary-value problem

191 The linear partial differential equation that governs, with respect to both time and space, the
 192 evolution of ^{13}C isotope in the liquid phase (i.e. enriched phase) in the rectifying section (see
 193 Fig. 2(b)) is given by [23, 27]:

$$(H_l + H_v) \frac{\partial N}{\partial t} = \left(\frac{L_r V_r}{K_r} \right) \frac{\partial^2 N}{\partial z^2} - [L_r(\alpha - 1) + P] \frac{\partial N}{\partial z} \quad (3)$$

194 where $H_l + H_v$ is the total carbon monoxide hold-up per unit volume in the rectifying section⁴,
 195 while K_r stands for the volumetric overall mass transfer coefficient in the rectifying section.

196 In the case of the stripping section (see Fig. 2(c)), the partial differential equation that
 197 governs the ^{13}C evolution in the liquid phase is given by :

$$(H_l + H_v) \frac{\partial N}{\partial t} = \left(\frac{L_s V_s}{K_s} \right) \frac{\partial^2 N}{\partial z^2} - [L_s(\alpha - 1) - W] \frac{\partial N}{\partial z} \quad (4)$$

198 where K_s is the volumetric overall mass transfer coefficient in the stripping section.

199 In order to solve (3) and (4) it is necessary to define the initial condition and the boundary
 200 conditions [37, 38]. The time-space domain of (3) and (4) is determined by the duration of the
 201 isotope separation process and by the length of the column.

202 The initial condition in both cases is represented by the desired isotope concentration at the
 203 moment of time $t = 0$ and it is given by the natural abundance of ^{13}C :

$$N(z, t = 0) = N_0 \quad (5)$$

204 The boundary conditions are given by the desired isotope evolution at height $z = 0$ (feeding
 205 point) and at the ends of the column, i.e. the bottom of the column in the case of the rectifying
 206 section ($z = Z_r$) and the top of the column in the case of the stripping section ($z = Z_s$).

207 Since during the extraction regime, the feeding is continuous and the raw material is repre-
 208 sented by carbon monoxide with a natural abundance of ^{13}C , the boundary condition at height
 209 $z = 0$ is given by:

$$N(z = 0, t) = N_0 \quad (6)$$

210 By integrating (3) with respect to height, we obtain:

$$\int (H_l + H_v) \frac{\partial N}{\partial t} dz + C_i = \left(\frac{L_r V_r}{K_r} \right) \frac{\partial N}{\partial z} - [L_r(\alpha - 1) + P] N \quad (7)$$

211 where C_i is an integration constant. The general form of (7) is referred to in [23, 24] as the
 212 *transport equation* and it relates the amount of the desired isotope carried along a column to the
 213 gradient of the mole fraction [24, 62]:

$$\mathcal{T} = [L_r(\alpha - 1) + P] N - \left(\frac{L_r V_r}{K_r} \right) \frac{\partial N}{\partial z} \quad (8)$$

⁴Since the hold-up is distributed homogeneously in the distillation column, the total carbon monoxide hold-up per unit volume in the rectifying section is equal to the total carbon monoxide hold-up per unit volume in the stripping section and is equal to the total carbon monoxide hold-up per unit volume in the column.

where \mathcal{T} stands for the desired isotope flow rate. At the end of the isotope separation column, we have [23, 24, 63]:

$$\mathcal{T} = NP \quad (9)$$

From (8) and (9) we obtain the boundary condition at the end of the rectifying section:

$$N(z = Z_r, t) = \frac{V_r}{K_r(\alpha - 1)} \frac{\partial N}{\partial z} \quad (10)$$

Analogously, the boundary condition at the end of the stripping section is given by:

$$N(z = Z_s, t) = \frac{V_s}{K_s(\alpha - 1)} \frac{\partial N}{\partial z} \quad (11)$$

Below we will use the following notations:

$$\eta_r \equiv \frac{(H_l + H_v)K_r}{L_r V_r} \quad (12)$$

$$\theta_r \equiv \frac{K_r(\alpha - 1)}{2V_r} \quad (13)$$

$$\psi_r \equiv \frac{P}{L_r(\alpha - 1)} \quad (14)$$

Using (12), (13), and (14), (3) can be written as:

$$\eta_r \frac{\partial N}{\partial t} = \frac{\partial^2 N}{\partial z^2} - 2\theta_r(1 + \psi_r) \frac{\partial N}{\partial z} \quad (15)$$

and the boundary condition (10) becomes:

$$N(z = Z_r, t) = \frac{1}{2\theta_r} \frac{\partial N}{\partial z} \quad (16)$$

For the stripping section, the analogous notations are:

$$\eta_s \equiv \frac{(H_l + H_v)K_s}{L_s V_s} \quad (17)$$

$$\theta_s \equiv \frac{K_s(\alpha - 1)}{2V_s} \quad (18)$$

$$\psi_s \equiv \frac{-W}{L_s(\alpha - 1)} \quad (19)$$

and (4) can be written as:

$$\eta_s \frac{\partial N}{\partial t} = \frac{\partial^2 N}{\partial z^2} - 2\theta_s(1 + \psi_s) \frac{\partial N}{\partial z} \quad (20)$$

while the boundary condition (11) becomes:

$$N(z = Z_s, t) = \frac{1}{2\theta_s} \frac{\partial N}{\partial z} \quad (21)$$

It can be seen that the relations for the stripping section are similar to the relations for the rectifying section.

226 3.2. Laplace transform

227 By applying the Laplace transform, the partial differential equation (15) turns into:

$$\eta_r [sG(z, s) - N_0] = \frac{d^2}{dz^2} G(z, s) - 2\theta_r(1 + \psi_r) \frac{d}{dz} G(z, s) \quad (22)$$

228 while the boundary conditions (6) and (16) become:

$$G(0, s) = \frac{N_0}{s} \quad (23)$$

$$G(Z_r, s) = \frac{1}{2\theta_r} \frac{d}{dz} G(Z_r, s) \quad (24)$$

229 where:

$$G(z, s) = \mathcal{L}\{N(z, t)\} = \int_0^\infty N(z, t) e^{-st} dt \quad (25)$$

230 Since the independent variable of (22) is the height z , while s is a parameter [60, 64], in the
 231 following we will use the simpler notation $G(z)$ instead of $G(z, s)$. The relation (22) can then be
 232 written as:

$$\frac{d^2}{dz^2} G(z) - 2\theta_r(1 + \psi_r) \frac{d}{dz} G(z) - \eta_r s G(z) = -\eta_r N_0 \quad (26)$$

233 It can be seen that (26) is an homogeneous linear ODE of the second order [65, 66].

234 The complementary equation of (26) is:

$$\frac{d^2}{dz^2} G(z) - 2\theta_r(1 + \psi_r) \frac{d}{dz} G(z) - \eta_r s G(z) = 0 \quad (27)$$

235 So the solution of (26) has the following form:

$$G(z) = G_p(z) + G_g(z) \quad (28)$$

236 where G_p is the particular solution of (26) and G_g is the general solution of (27).

237 In order to find the particular solution of (26) we will choose the *method of undetermined*
 238 *coefficients*. Therefore, the particular solution, which is a polynomial of the same degree as the
 239 non homogeneous term, will verify (26). It can be easily found that the particular solution G_p
 240 is given by:

$$G_p = \frac{N_0}{s} \quad (29)$$

241 The *auxiliary equation* of (27) is [65]:

$$r^2 - 2\theta_r(1 + \psi_r)r - \eta_r s = 0 \quad (30)$$

242 with roots:

$$r_1 = \frac{2\theta_r(1 + \psi_r) + \sqrt{4\theta_r^2(1 + \psi_r)^2 + 4\eta_r s}}{2} \quad (31)$$

$$r_2 = \frac{2\theta_r(1 + \psi_r) - \sqrt{4\theta_r^2(1 + \psi_r)^2 + 4\eta_r s}}{2} \quad (32)$$

243 Hence, the general solution of (27) is given by [66, 67]:

$$G_g(z) = C_1 e^{r_1 z} + C_2 e^{r_2 z} \quad (33)$$

244 where C_1 and C_2 are constants. The solution of (26) follows:

$$G(z) = G_p(z) + G_g(z) = \frac{N_0}{s} + C_1 e^{r_1 z} + C_2 e^{r_2 z} \quad (34)$$

245 The constants C_1 and C_2 can be found by replacing (34) in (23) and (24).

246 For $z = 0$, from (34) and (23) we obtain:

$$G(0) = \frac{N_0}{s} = \frac{N_0}{s} + C_1 e^0 + C_2 e^0 \quad (35)$$

247 whence:

$$C_1 = -C_2 \equiv C \quad (36)$$

248 For $z = Z_r$, from (34) and (24) we obtain:

$$2\theta_r G(Z_r) - \frac{d}{dz} G(Z_r) = 0 \quad (37)$$

249 whence, referring to (34) and (36):

$$G(Z_r) = \frac{N_0}{s} + C e^{r_1 Z_r} - C e^{r_2 Z_r} \quad (38)$$

250 The term $\frac{d}{dz} G(Z_r)$ is given by:

$$\frac{d}{dz} G(Z_r) = r_1 C e^{r_1 Z_r} - r_2 C e^{r_2 Z_r} \quad (39)$$

251 From (37), (38), and (39) we obtain:

$$C \left(r_1 e^{r_1 Z_r} - r_2 e^{r_2 Z_r} \right) - 2\theta_r C \left(e^{r_1 Z_r} - e^{r_2 Z_r} \right) = 2\theta_r \frac{N_0}{s} \quad (40)$$

252 In the following we will define the term $\beta(s)$ as:

$$\beta(s) \equiv \sqrt{\theta_r^2(1 + \psi_r)^2 + \eta_r s} \quad (41)$$

253 The roots of the auxiliary equation can then be written as:

$$r_1 = \theta_r(1 + \psi_r) + \beta(s) \quad (42)$$

$$r_2 = \theta_r(1 + \psi_r) - \beta(s) \quad (43)$$

254 Using (42) and (43), (40) becomes:

$$C e^{\theta_r(1+\psi_r)Z_r} \left\{ [\theta_r(1+\psi_r)+\beta(s)] e^{\beta(s)Z_r} - [\theta_r(1+\psi_r)-\beta(s)] e^{-\beta(s)Z_r} - 2\theta_r \left(e^{\beta(s)Z_r} - e^{-\beta(s)Z_r} \right) \right\} = 2\theta_r \frac{N_0}{s} \quad (44)$$

255 whence the constant C follows:

$$C = 2\theta_r \frac{N_0}{s} e^{-\theta_r(1+\psi_r)Z_r} \frac{1}{\beta(s)(e^{\beta(s)Z_r} + e^{-\beta(s)Z_r}) - \theta_r(1 + \psi_r)(e^{\beta(s)Z_r} - e^{-\beta(s)Z_r})} \quad (45)$$

256 Using Euler's formula [43]:

$$e^{ix} = \cos(x) + i \sin(x) \quad (46)$$

257 whence:

$$\cos(x) = \frac{1}{2}(e^{ix} + e^{-ix}) \quad (47)$$

$$\sin(x) = \frac{1}{2i}(e^{ix} - e^{-ix}) \quad (48)$$

258 we can write:

$$(e^{\beta(s)Z_r} + e^{-\beta(s)Z_r}) = 2 \cos(i\beta(s)Z_r) \quad (49)$$

$$(e^{\beta(s)Z_r} - e^{-\beta(s)Z_r}) = (-2i) \sin(i\beta(s)Z_r) \quad (50)$$

259 Referring to (49) and (50), (45) turns into:

$$C = C_1 = -C_2 = 2\theta_r \frac{N_0}{s} e^{-\theta_r(1+\psi_r)Z_r} \frac{1}{2[\beta(s) \cos(i\beta(s)Z_r) - \theta_r(1 - \psi_r)(-i) \sin(i\beta(s)Z_r)]} \quad (51)$$

260 The solution of (26) follows:

$$G(z) = \frac{N_0}{s} + C e^{\theta_r(1+\psi_r)z} (-2i) \sin(i\beta(s)z) \quad (52)$$

261 By defining:

$$\gamma(s) \equiv i\beta(s) \quad (53)$$

262 we can write (52) as:

$$G(z, s) = \frac{N_0}{s} + 2\theta_r \frac{N_0}{s} e^{\theta_r(1+\psi_r)(z-Z_r)} \frac{\sin(\gamma(s)z)}{\gamma(s) \cos(\gamma(s)Z_r) - \theta_r(1 - \psi_r) \sin(\gamma(s)Z_r)} \quad (54)$$

263 Analogously, in the case of the striping section we obtain:

$$G(z, \tilde{s}) = \frac{N_0}{\tilde{s}} + 2\theta_s \frac{N_0}{\tilde{s}} e^{\theta_s(1+\psi_s)(z-Z_s)} \frac{\sin(\gamma(\tilde{s})z)}{\gamma(\tilde{s}) \cos(\gamma(\tilde{s})Z_s) - \theta_s(1-\psi_s) \sin(\gamma(\tilde{s})Z_s)} \quad (55)$$

264 where

$$\gamma(\tilde{s}) \equiv i\sqrt{\theta_s^2(1+\psi_s)^2 + \eta_s \tilde{s}} \quad (56)$$

265 By applying the inverse Laplace transform to (54) and (55) we obtain the analytical solution
266 of the isotope separation process.

267 3.3. Inverse Laplace transform and the analytical solution of the isotope separation process

268 In order to find the inverse of the Laplace transform of a function, one can use the contour
269 integration, the convolution theorem, tables of integral transforms, or Heaviside's expansion
270 theorem [41, 44, 45, 68–71].

271 Given the complexity of (54) and (55) it is convenient to use the generalized Heaviside's
272 expansion theorem [68, 72, 73] for finding the inverse Laplace transform.

273 In order to apply the Heaviside's expansion theorem we will rewrite (54) as:

$$G(z, s) = \frac{N_0}{s} + \frac{2\theta_r N_0 e^{\theta_r(1+\psi_r)(z-Z_r)} \frac{\sin(\gamma(s)z)}{\sin(\gamma(s)Z_r)}}{s \left[\gamma(s) \frac{1}{\tan(\gamma(s)Z_r)} - \theta_r(1-\psi_r) \right]} \quad (57)$$

274 By defining

$$g(s) \equiv \gamma(s) \frac{1}{\tan(\gamma(s)Z_r)} - \theta_r(1-\psi_r) \quad (58)$$

275 the relation (57) becomes:

$$G(z, s) = \frac{N_0 \left[g(s) + 2\theta_r e^{\theta_r(1+\psi_r)(z-Z_r)} \frac{\sin(\gamma(s)z)}{\sin(\gamma(s)Z_r)} \right]}{sg(s)} \equiv \frac{q(s)}{p(s)} \quad (59)$$

276 where

$$q(s) \equiv N_0 \left[g(s) + 2\theta_r e^{\theta_r(1+\psi_r)(z-Z_r)} \frac{\sin(\gamma(s)z)}{\sin(\gamma(s)Z_r)} \right] \quad (60)$$

277 and

$$p(s) \equiv sg(s) \quad (61)$$

278 The zeros of $p(s)$ are $s_1 = 0$ and the solutions of:

$$g(s) = 0 \quad (62)$$

279 or

$$\tan(\gamma(s)Z_r) = \frac{\gamma(s)}{\theta_r(1-\psi_r)} \quad (63)$$

280 The relation (63) is a *transcendental equation* and its solution will be discussed in Section
281 3.4.

282 In the case of the stripping section, the analogous transcendental equation is:

$$\tan(\gamma(\tilde{s})Z_s) = \frac{\gamma(\tilde{s})}{\theta_s(1-\psi_s)} \quad (64)$$

283 For finding the function that describes the evolution of the concentration of the desired
284 isotope in the rectifying section, we will apply the Heaviside's expansion theorem to (59). Thus,
285 the function N will have the form [41, 60, 72]:

$$N(z, t) = \sum_{k=1}^n a_k e^{s_k t} \quad (65)$$

286 where

$$a_1 = \lim_{s \rightarrow s_1} sG(z, s) \quad (66)$$

287 while

$$a_j = \frac{q(s_j)}{p'(s_j)} \quad (67)$$

288 where s_j , for $j = 2, 3, \dots, n$, are the solutions of (63).

289 **Theorem 1. *Final value theorem*** [59]. *If F is the Laplace transform of the function f , then:*

$$\lim_{s \rightarrow 0} sF(s) = \lim_{t \rightarrow \infty} f(t) \quad (68)$$

290 It can be seen that the value of the coefficient a_1 is the final value of the function N :

$$a_1 = \lim_{s \rightarrow 0} sG(z, s) = \lim_{t \rightarrow \infty} N(z, t) \quad (69)$$

291 By solving (66), using (68), we obtain the stationary value of the concentration of the desired
292 isotope at an arbitrary height z in the rectifying section:

$$\lim_{t \rightarrow \infty} N(z, t) = N_0 \frac{e^{2\theta_r(1+\psi_r)z} + \psi_r e^{2\theta_r(1+\psi_r)Z_r}}{1 + \psi_r e^{2\theta_r(1+\psi_r)Z_r}} \quad (70)$$

293 Analogously, the stationary value of the concentration of the desired isotope at an arbitrary
294 height z in the stripping section is given by:

$$\lim_{t \rightarrow \infty} N(z, t) = N_0 \frac{e^{2\theta_s(1+\psi_s)z} + \psi_s e^{2\theta_s(1+\psi_s)Z_s}}{1 + \psi_s e^{2\theta_s(1+\psi_s)Z_s}} \quad (71)$$

295 Since s_j are the solution of $g(s) = 0$, (60) yields:

$$q(s_j) = N_0 \left[2\theta_r e^{\theta_r(1+\psi_r)(z-Z_r)} \frac{\sin(\gamma(s_j)z)}{\sin(\gamma(s_j)Z_r)} \right] \quad (72)$$

296 and

$$p'(s_j) = s_j g'(s_j) \quad (73)$$

297 By derivation with respect to s , (58) becomes:

$$g'(s_j) = \frac{\eta_r Z_r}{2} - \frac{\eta_r}{2(\gamma(s_j))^2} \theta_r (1 - \psi_r) [1 - Z_r \theta_r (1 - \psi_r)] \quad (74)$$

298 From (72) and (74) we obtain the value of the coefficient a_j :

$$a_j = \frac{N_0 \left[2\theta_r e^{\theta_r(1+\psi_r)(z-Z_r)} \frac{\sin(\gamma(s_j)z)}{\sin(\gamma(s_j)Z_r)} \right]}{s_j \left\{ \frac{\eta_r Z_r}{2} - \frac{\eta_r}{2(\gamma(s_j))^2} \theta_r (1 - \psi_r) [1 - Z_r \theta_r (1 - \psi_r)] \right\}} \quad (75)$$

299 The analytical solution of the isotope separation process, in the rectifying section, follows:

$$N(z, t) = N_0 \frac{e^{2\theta_r(1+\psi_r)z} + \psi_r e^{2\theta_r(1+\psi_r)Z_r}}{1 + \psi_r e^{2\theta_r(1+\psi_r)Z_r}} + \sum_{j=2}^n \frac{N_0 \left[2\theta_r e^{\theta_r(1+\psi_r)(z-Z_r)} \frac{\sin(\gamma(s_j)z)}{\sin(\gamma(s_j)Z_r)} \right]}{s_j \left\{ \frac{\eta_r Z_r}{2} - \frac{\eta_r}{2(\gamma(s_j))^2} \theta_r (1 - \psi_r) [1 - Z_r \theta_r (1 - \psi_r)] \right\}} e^{s_j t} \quad (76)$$

300 where θ_r , ψ_r , and $\gamma(s_j)$ are the parameters of the isotope separation process in the rectifying
 301 section (see (12), (13), (14), and (53)), while s_j , for $j = 2, 3, \dots, n$, are the solutions of the
 302 transcendental equation (63).

303 Analogously, in the case of the stripping section, the analytical solution is given by the similar
 304 relation:

$$N(z, t) = N_0 \frac{e^{2\theta_s(1+\psi_s)z} + \psi_s e^{2\theta_s(1+\psi_s)Z_s}}{1 + \psi_s e^{2\theta_s(1+\psi_s)Z_s}} + \sum_{j=2}^{\tilde{n}} \frac{N_0 \left[2\theta_s e^{\theta_s(1+\psi_s)(z-Z_s)} \frac{\sin(\gamma(\tilde{s}_j)z)}{\sin(\gamma(\tilde{s}_j)Z_s)} \right]}{\tilde{s}_j \left\{ \frac{\eta_s Z_s}{2} - \frac{\eta_s}{2(\gamma(\tilde{s}_j))^2} \theta_s (1 - \psi_s) [1 - Z_s \theta_s (1 - \psi_s)] \right\}} e^{\tilde{s}_j t} \quad (77)$$

305 In this case, θ_s , ψ_s , and $\gamma(\tilde{s}_j)$ are the parameters of the isotope separation process in the
 306 stripping section (see (17), (18), (19), and (53)), while \tilde{s}_j , for $j = 2, 3, \dots, \tilde{n}$, are the solutions of
 307 the transcendental equation (64).

308 Using (76) and (77) one can determine the concentration of the desired isotope at any height
 309 z and at any moment of time t , with respect to plant parameters like the hold-up, liquid and
 310 vapor molar flow rate, separation factor, and the height of the distillation column.

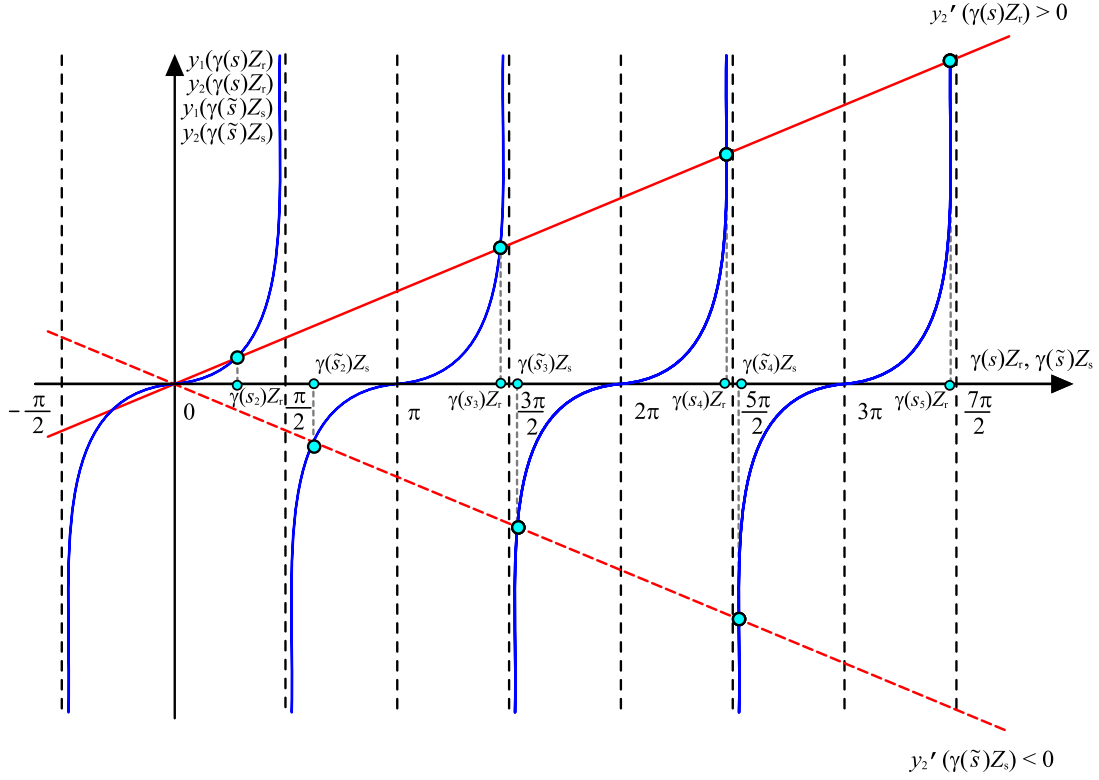


Figure 3: Graphical representation of the functions $y_1(\gamma(s)Z_r)$, $y_1(\gamma(\tilde{s})Z_s)$ and $y_2(\gamma(s)Z_r)$, $y_2(\gamma(\tilde{s})Z_s)$.

3.4. Solving the transcendental equations (63) and (64)

In our case, (63) can be written as:

$$\tan(\gamma(s)Z_r) = \frac{(\gamma(s)Z_r)}{\theta_r Z_r (1 - \psi_r)} \quad (78)$$

Both sides of (78) can be expressed as two functions of the same argument:

$$y_1(\gamma(s)Z_r) = \tan(\gamma(s)Z_r) \quad (79)$$

$$y_2(\gamma(s)Z_r) = \frac{(\gamma(s)Z_r)}{Z_r \theta_r (1 - \psi_r)} \quad (80)$$

Fig. 3 shows the graphical representation of the functions $y_1(\gamma(s)Z_r)$, $y_1(\gamma(\tilde{s})Z_s)$ and $y_2(\gamma(s)Z_r)$, $y_2(\gamma(\tilde{s})Z_s)$. Since the height gradient is positive in the rectifying section and negative in the stripping section, $y_2'(\gamma(s)Z_r) > 0$, while $y_2'(\gamma(\tilde{s})Z_s) < 0$.

The solutions of (78) are given by the points for which the following is true:

$$y_1(\gamma(s_j)Z_r) = y_2(\gamma(s_j)Z_r) \quad (81)$$

318 or, in other words, in the intersection points of the two functions.

319 By knowing the value of $(\gamma(s_j)Z_r)$, where $j = 2, 3, \dots, n$, one can find the solutions of (62),
 320 and the analytic solution of the isotope separation process in the rectifying section becomes
 321 completely determined. Knowing that (see (53)):

$$(\gamma(s_j)Z_r) = i \left(\sqrt{\theta_r^2(1 + \psi_r)^2 + \eta_r s_j} \right) Z_r \quad (82)$$

322 we obtain the solutions of (62):

$$s_j = - \left[\frac{(\gamma(s_j)Z_r)^2 + Z_r^2 \theta_r^2 (1 + \psi_r)^2}{\eta_r Z_r^2} \right] \quad (83)$$

323 Since η_r is a positive quantity (see (12)) one can see from (83) that $s_j < 0$. Thus, the terms
 324 in the infinite series (see (76)) are transient and the series converges.

325 Analogously, in the case of the stripping section we obtain:

$$\tilde{s}_j = - \left[\frac{(\gamma(\tilde{s}_j)Z_s)^2 + Z_s^2 \theta_s^2 (1 + \psi_s)^2}{\eta_s Z_s^2} \right] \quad (84)$$

326 For determining the intersection points $(\gamma(s_j)Z_r)$ and $(\gamma(\tilde{s}_j)Z_s)$ as plotted in Fig. 3 we have
 327 used the MATLAB function *fzero*. The function *fzero* find the roots of a continuous function of
 328 one variable around an arbitrary point [74, 75].

329 4. Validation of the analytical solution of the isotope separation process

330 Usually, the only points where the isotopic concentration is measurable are at the bottom and
 331 at the top of the column. In order to validate the analytical solution, we will use (76) and (77)
 332 written for the boundary conditions $z = Z_r$ (the end of the rectifying section, i.e. the bottom of
 333 the column) and $z = Z_s$ (the end of the stripping section, i.e. the top of the column).

334 In the following we will refer to three isotope separation experiments carried using the exper-
 335 imental pilot-scale plant developed at the National Institute for Research and Development of
 336 Isotopic and Molecular Technologies in Cluj-Napoca, Romania. The three experiments were con-
 337 ducted in total-reflux regime for different electrical powers that supplied the heating resistance,
 338 i.e. 24 W, 27 W, and 29 W.

339 The analytical solution (76) written for $z = Z_r$ is given by:

$$N(z = Z_r, t) = N_0 \frac{(1 + \psi_r) e^{2\theta_r(1 + \psi_r)Z_r}}{1 + \psi_r e^{2\theta_r(1 + \psi_r)Z_r}} + \sum_{j=2}^n \frac{N_0 2\theta_r}{s_j \left\{ \frac{\eta_r Z_r}{2} - \frac{\eta_r}{2(\gamma(s_j))^2} \theta_r (1 - \psi_r) [1 - Z_r \theta_r (1 - \psi_r)] \right\}} e^{s_j t} \quad (85)$$

Since the experiments were conducted in total-reflux regime, no withdrawal was performed and therefore:

$$F = P = W = 0 \quad (86)$$

whence (see (14)) $\psi_r = 0$. Thus, (85) becomes:

$$N(z = Z_r, t) = N_0 e^{2\theta_r Z_r} + \sum_{j=2}^n \frac{N_0 2\theta_r}{s_j \left[\frac{\eta_r Z_r}{2} - \frac{\eta_r \theta_r}{2(\gamma(s_j))^2} (1 - Z_r \theta_r) \right]} e^{s_j t} \quad (87)$$

Analogously, the analytical solution written for the boundary condition $z = Z_s$ and the total-reflux condition $\psi_s = 0$ is given by:

$$N(z = Z_s, t) = N_0 e^{2\theta_s Z_s} + \sum_{j=2}^{\tilde{n}} \frac{N_0 2\theta_s}{\tilde{s}_j \left[\frac{\eta_s Z_s}{2} - \frac{\eta_s \theta_s}{2(\gamma(\tilde{s}_j))^2} (1 - Z_s \theta_s) \right]} e^{\tilde{s}_j t} \quad (88)$$

The relations (87) and (88) describe the evolution of the mole fraction of the desired isotopic compound at the bottom and at the top of the column with respect to process parameters like hold-up, internal molar flow rates, height of the column, and the separation factor.

4.1. Parameters of the analytical solution of the isotope separation process

Since the plant's configuration consists of one distillation column with a single reboiler, the vapor molar flow rate in the rectifying section is equal to the vapor molar flow rate in the stripping section ($V_r = V_s$). The vapor internal stream is determined by the electrical power that supplied the heating resistance and the heat transfer through the multilayered vacuum jacket [76–78]. The liquid molar flow rate is determined by the total-reflux condition. The total hold-up in the column $H_l + H_v$ is determined by measuring the quantity of raw material fed to the column during the operations prior to the beginning of each experiment.

Naturally, during the total-reflux experiment, the raw material will have, at a certain height z , in steady state, the natural isotopic abundance (N_0). When the product is represented by the less volatile component, under the height corresponding to the natural isotopic abundance (toward to the bottom of the column) the concentration of the desired isotope will be higher than its natural abundance, while above this height, the isotope concentration will be lower than its natural abundance. Therefore, the total-reflux regime can be analyzed as a particular case of the extraction regime, when no withdrawal is performed and thus, the feed flow rate F , the product flow rate P , and the waste flow rate W are zero, and the feed point will correspond to the height for which the raw material isotopic concentration corresponds to the natural abundance (see Fig. 2(a), Fig. 2(b), and Fig. 2(c)).

366 The rate of transfer of the heavy isotopic compound (the product) to the liquid phase across
 367 the interface per unit volume, in the rectifying section, is given by [23, 27]:

$$\tau_r = -K_r[(N - n) - n(\alpha - 1)(1 - N)] \quad (89)$$

368 where the separation factor α is:

$$\alpha = \frac{\frac{N}{1-N}}{\frac{n}{1-n}} \quad (90)$$

369 Analogously, the rate of transfer of the light isotopic compound to the vapor phase in the
 370 stripping section is given by:

$$\tau'_s = -K_s[(n' - N') - N'(\alpha' - 1)(1 - n')] \quad (91)$$

371 where n' and N' correspond to the mole fraction of the light isotopic compound in the vapor
 372 phase, while α' is:

$$\alpha' = \frac{\frac{n'}{1-n'}}{\frac{N'}{1-N'}} > 1 \quad (92)$$

373 Since during the total-reflux regime no products are withdrawn and the feed flow rate is zero,
 374 the rate of transfer of the heavy isotopic compound to the liquid phase in the stripping section
 375 will be equal but in opposite sign to the rate of transfer of the heavy isotopic compound to the
 376 liquid phase in the rectifying section:

$$\tau_s = \tau'_s = -\tau_r \quad (93)$$

377 In our case, the raw material corresponds to a binary mixture, and thus [27, 32]:

$$n' = 1 - n \quad (94)$$

$$N' = 1 - N \quad (95)$$

$$\alpha' = \alpha \quad (96)$$

378 The description of τ_s follows:

$$\tau_s = -K_s[(N - n) - n(\alpha - 1)(1 - N)] \quad (97)$$

379 From (89), (93), and (97) we obtain:

$$K_r = K_s \quad (98)$$

380 Previously we have determined the stationary value of the concentration of the desired isotope
 381 at an arbitrary height z in the separation column (see (70) and (71)). Usually, the only points

382 were the isotopic concentration is measurable are at the top of the column and at the bottom of
 383 the column. By referring to (70) and (71) and knowing that the experiments were conducted in
 384 total-reflux regime and therefore $\psi_r = \psi_s = 0$ (see (14) and (19)) we obtain the stationary value
 385 of the concentration at the end of the rectifying section $z = Z_r$ (bottom of the column) and at
 386 the end of the stripping section $z = Z_s$ (top of the column):

$$\lim_{t \rightarrow \infty} N(Z_r, t) = N_0 e^{2\theta_r Z_r} \quad (99)$$

$$\lim_{t \rightarrow \infty} N(Z_s, t) = N_0 e^{2\theta_s Z_s} \quad (100)$$

387 Since the stationary values of the desired isotope concentration are determined experimentally,
 388 by referring to (13) and (18), the description of K_r and K_s follows:

$$K_r = \frac{V_r}{(\alpha - 1)Z_r} \ln \left(\frac{\lim_{t \rightarrow \infty} N(Z_r, t)}{N_0} \right) \quad (101)$$

$$K_s = \frac{V_s}{(\alpha - 1)Z_s} \ln \left(\frac{\lim_{t \rightarrow \infty} N(Z_s, t)}{N_0} \right) \quad (102)$$

389 From (98), (101), and (102), and knowing that $Z_c = Z_r - Z_s$ is possible to determine the
 390 height of the rectifying and stripping section of a distillation column that operates in total-reflux
 391 regime:

$$Z_r = Z_c \frac{\ln \left(\frac{\lim_{t \rightarrow \infty} N(Z_r, t)}{N_0} \right)}{\ln \left(\frac{\lim_{t \rightarrow \infty} N(Z_r, t)}{\lim_{t \rightarrow \infty} N(Z_s, t)} \right)} \quad (103)$$

$$Z_s = Z_c \frac{\ln \left(\frac{\lim_{t \rightarrow \infty} N(Z_s, t)}{N_0} \right)}{\ln \left(\frac{\lim_{t \rightarrow \infty} N(Z_r, t)}{\lim_{t \rightarrow \infty} N(Z_s, t)} \right)} \quad (104)$$

392 Since the heights of the rectifying and stripping section (Z_r and Z_s) depend on measurable
 393 parameters like the total height of the column Z_c , the stationary values of the concentration at
 394 the ends of the column, and on the natural abundance of ^{13}C , one can determine the constant
 395 concentration point Z_0 as being at height Z_s from the top of the column or Z_r from the bottom
 396 of the column (see Figure 2(a)).

397 Knowing the vapor and liquid molar flow rates, the total hold-up in the column ($H_l + H_v$),
 398 the heights of the rectifying and stripping section (Z_r and Z_s), and the separation factor (α), it
 399 is possible to determine the parameters of the analytical solution and, thus, to obtain the isotope
 400 distribution with respect to both time and height by computing (76) and (77).

Table 2: Parameters of the analytical solution and the heights of the rectifying and stripping section in the case of all three isotope separation experiments.

| $P_{\text{electrical}}$ (W) | $\eta_r = \eta_s$ $\left(\frac{\text{s}}{\text{m}^2}\right)$ | $\theta_r = \theta_s$ $\left(\frac{1}{\text{m}}\right)$ | $\psi_r = \psi_s$ (-) | Z_r (m) | Z_s (m) |
|--------------------------------|---|--|--------------------------|--------------|--------------|
| 24 | 12198.062 | 0.168 | 0 | 2.390 | -4.610 |
| 27 | 9664.195 | 0.143 | 0 | 2.956 | -4.044 |
| 29 | 9798.104 | 0.152 | 0 | 2.884 | -4.116 |

Table 3: The values of $(\gamma(s_j)Z_r)$ and $(\gamma(\tilde{s}_j)Z_s)$ when $j = 2, 3, 4, 5$, and 6 in the case of all three isotope separation experiments.

| $P_{\text{electrical}}$ (W) | $(\gamma(s_2)Z_r)$ (-) | $(\gamma(s_3)Z_r)$ (-) | $(\gamma(s_4)Z_r)$ (-) | $(\gamma(s_5)Z_r)$ (-) | $(\gamma(s_6)Z_r)$ (-) |
|--------------------------------|---------------------------|---------------------------|---------------------------|---------------------------|---------------------------|
| 24 | 1.262 | 4.625 | 7.802 | 10.958 | 14.108 |
| 27 | 1.242 | 4.621 | 7.799 | 10.956 | 14.107 |
| 29 | 1.226 | 4.617 | 7.797 | 10.955 | 14.105 |

| $P_{\text{electrical}}$ (W) | $(\gamma(\tilde{s}_2)Z_s)$ (-) | $(\gamma(\tilde{s}_3)Z_s)$ (-) | $(\gamma(\tilde{s}_4)Z_s)$ (-) | $(\gamma(\tilde{s}_5)Z_s)$ (-) | $(\gamma(\tilde{s}_6)Z_s)$ (-) |
|--------------------------------|-----------------------------------|-----------------------------------|-----------------------------------|-----------------------------------|-----------------------------------|
| 24 | 1.949 | 4.870 | 7.951 | 11.065 | 14.191 |
| 27 | 1.870 | 4.831 | 7.926 | 11.047 | 14.177 |
| 29 | 1.891 | 4.841 | 7.933 | 11.052 | 14.181 |

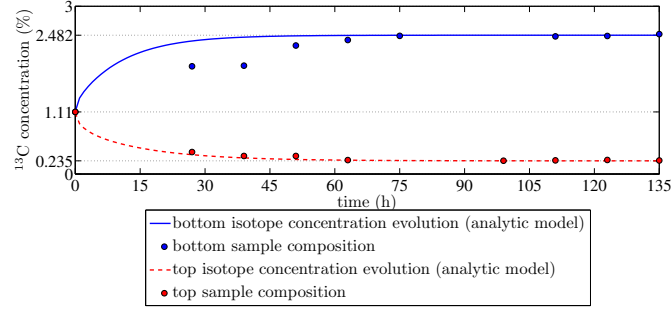
Table 2 summarizes the parameters of the analytical solution, as well as the heights of the rectifying section and stripping section in the case of the three isotope separation experiments.

The first five values⁵ of $(\gamma(s_j)Z_r)$ and $(\gamma(\tilde{s}_j)Z_s)$ are listed in Table 3.

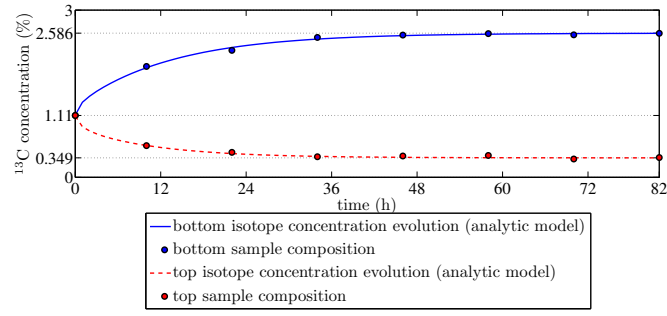
4.2. Assessment of the analytical solution of the isotope separation process

Fig. 4(a), 4(b), and 4(c) show the ^{13}CO mole fraction evolution at both ends of the distillation column in the case of the three isotope separation experiments. The results were obtained by computing the analytical solution described by (87) and (88). In addition, the measured values are also plotted.

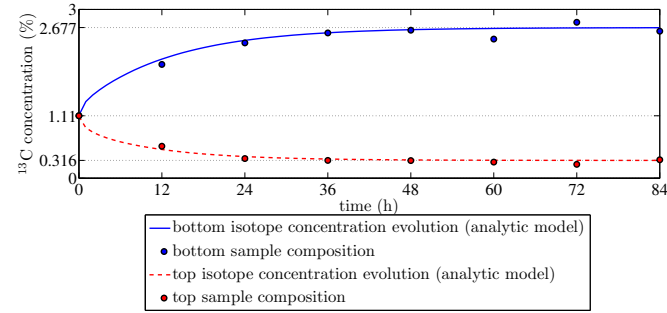
⁵For brevity, we remind that the first solution of the transcendental equations is indicated by the index $j = 2$.



(a) 24 W case.



(b) 27 W case.

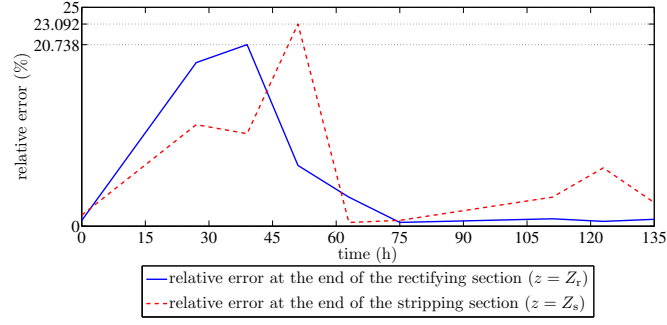


(c) 29 W case.

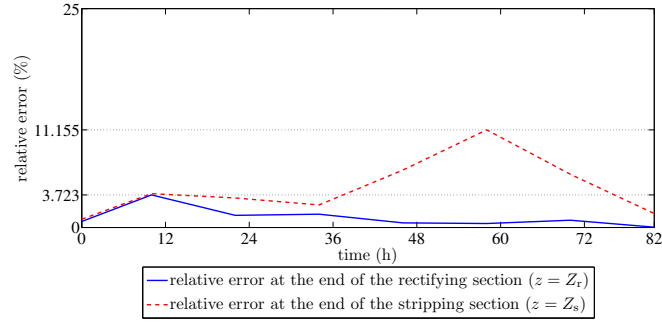
Figure 4: ^{13}C concentration evolution according to the analytical solution and ^{13}C concentrations achieved by the pilot-scale experimental plant.

409 Fig. 5(a), 5(b), and 5(c) show the relative error of the analytical solution at both ends of the
 410 separation column. Explicitly, in all three cases, the relative error was calculated using:

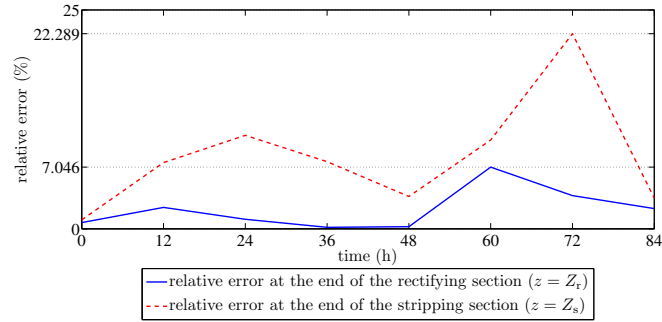
$$\zeta(z = Z_r, t) = \left| \frac{N_{\text{analytic}}(z = Z_r, t) - N_{\text{experimental}}(z = Z_r, t)}{N_{\text{analytic}}(z = Z_r, t)} \right| \quad (105)$$



(a) 24 W case.



(b) 27 W case.

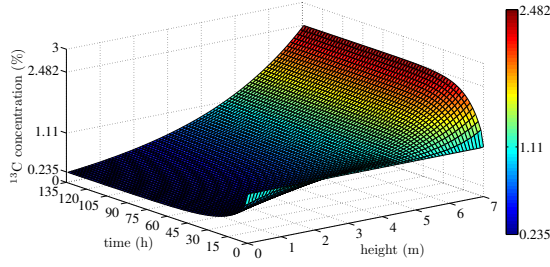


(c) 29 W case.

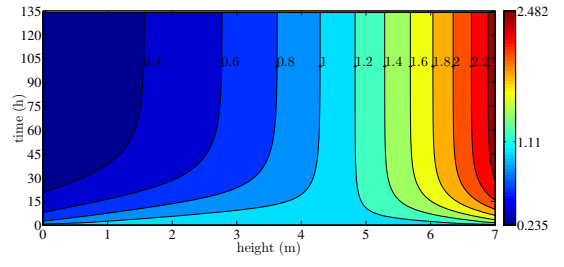
Figure 5: Relative errors between simulated and measured data at the end of the rectifying section (bottom of the column) and at the end of the stripping section (top of the column).

for the rectifying section. For the stripping section the relative error was calculated similarly.

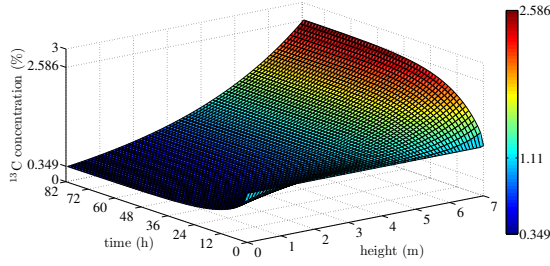
Fig. 6(a), 6(b), 6(c), 6(d), 6(e), and 6(f) show the ^{13}CO mole fraction distribution in the column with respect to both height and time. The isotope distribution was obtained by computing the analytical solution described by (76) and (77). The simulation results were obtained



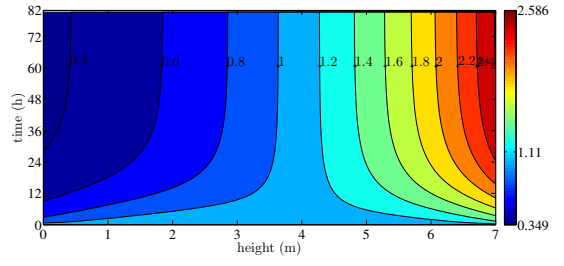
(a) ^{13}C isotope concentration distribution. The electrical power applied to the heater was 24 W.



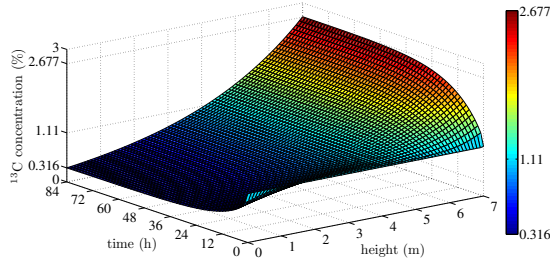
(b) ^{13}C isotope concentration distribution (contour view). The electrical power applied to the heater was 24 W.



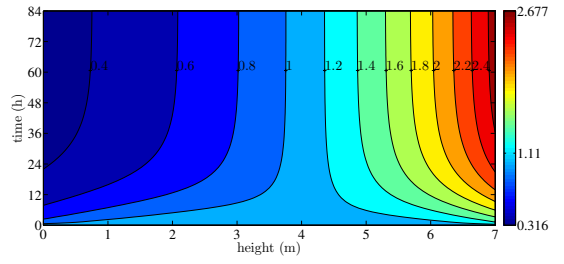
(c) ^{13}C isotope concentration distribution. The electrical power applied to the heater was 27 W.



(d) ^{13}C isotope concentration distribution (contour view). The electrical power applied to the heater was 27 W.



(e) ^{13}C isotope concentration distribution. The electrical power applied to the heater was 29 W.



(f) ^{13}C isotope concentration distribution (contour view). The electrical power applied to the heater was 29 W.

Figure 6: ^{13}C isotope concentration distribution with respect to time and height.

for a 70 discretization divisions applied to the space domain (i.e. a height step of 0.1 m) and a time step of 1800 s emphasizing that the isotopic concentration can be simulated at any moment of time and at any height. The simulation time was approximately 1.5 s in the case of all three experiments.

In Table 4 we have listed the values of the maximum and average relative error at the ends of the separation column, in the case of all three experiments.

Table 4: The values of the maximum and average relative error between simulated and measured data at the ends of the separation column.

| $P_{\text{electrical}}$ (W) | $\max(\zeta(z = Z_r, t))$ (%) | $\max(\zeta(z = Z_s, t))$ (%) | $\overline{\zeta(z = Z_r, t)}$ (%) | $\overline{\zeta(z = Z_s, t)}$ (%) |
|--------------------------------|----------------------------------|----------------------------------|---------------------------------------|---------------------------------------|
| 24 | 20.738 | 23.092 | 5.880 | 6.696 |
| 27 | 3.723 | 11.155 | 1.144 | 4.516 |
| 29 | 7.046 | 22.289 | 2.225 | 8.318 |

When the electrical power applied to the heater was 24 W, the average relative error at the bottom of the column was 5.8 %, while at the top of the column it was 6.6 %. When the electrical power was 27 W, the average relative error was 1.1 % at the bottom of the column and 4.5 % at the top of the column. In the case of 29 W, the average relative error was 2.2 % at the bottom and 8.3 % at the top of the column.

The volumetric overall mass transfer coefficient is determined by plant parameters such as the internal vapor molar flow rate V , the separation factor α , the heights of the rectifying and stripping sections of the distillation column (Z_r and Z_s), and to the steady-state values of the concentration achieved at the ends of the separation column. Using the results of Section 4, one can use interpolation to determine the volumetric overall mass transfer coefficient with respect to the above parameters, and thus, expensive experiments could be avoided.

5. Conclusions

Isotope separation processes have a coupled time-space nature and their inputs, outputs, and parameters can vary both in time and space. Modeling of such complex processes requires time and knowledge from a variety of fields. However, finding an appropriate analytic model eases the linking to the physics of the process and brings considerable advantages in understanding the subprocesses and the associated interactions. In this paper we have presented a modeling approach in order to find the analytic expression of a ^{13}C isotope separation process by cryogenic distillation of carbon monoxide. Firstly, after a short review of isotope separation processes, based on the partial differential equation that governs the isotope separation process, we have defined the initial-boundary-value problem. Using the Laplace transform, we have transformed the PDE into a linear homogeneous ODE. Next, we have determined the solution of the ODE and, by using Heaviside's expansion theorem, we have found the inverse Laplace transform. The analytic model

of the isotope separation process followed. The only points where the isotopic concentration is measurable in practice are at the ends of the distillation column. In order to validate the analytic model, we have simulated the evolution of the desired isotope in total-reflux regime, at both the bottom and the top of the column, and compared it with experimental data gathered from an experimental ^{13}C isotope separation plant. The three experiments were conducted in total-reflux regime for different electrical powers that supplied the heating resistance, i.e. 24 W, 27 W, and 29 W. When the electrical power was 24 W, the average relative error at the bottom of the column was 5.8 %, while at the top of the column it was 6.6 %. In the case of 27 W, the average relative errors were 1.1 % at the bottom of the column and 4.5 % at the top of the column. When the electrical power was 29 W, the average relative error at the bottom of the column was 2.2 % and 8.3 % at the top of the column, showing that the analytic model is a valid modeling approach.

Future studies will involve withdrawal-regime isotope separation experiments, in order to further analyze the analytic model and the volumetric overall mass transfer coefficient. Also, the effects of the packing over the hold-up and response time, internal flow rates, and production will be treated in order to optimize the isotope separation process. Using the obtained analytic model, the effects of the hydrodynamical variables fluctuations over the separation process will be studied from the control point of view.

Acknowledgments

This paper was supported by the project "Doctoral studies in engineering sciences for developing the knowledge based society-SIDOC" contract no. POSDRU/88/1.5/S/60078, project co-funded from European Social Fund through Sectorial Operational Program Human Resources 2007-2013.

References

- [1] G. Faure and T.M. Mensing. *Isotopes. Principles and Applications*. John Wiley and Sons, Hoboken, third edition, 2005.
- [2] B.J. Peterson, R.W. Howarth, and R.H. Garritt. Multiple stable isotopes used to trace the flow of organic matter in estuarine food webs. *Science*, 227(4692):1361–1363, 1985.
- [3] W.W. Cleland. The use of isotope effects to determine enzyme mechanisms. *The Journal of Biological Chemistry*, 278(52):51975–51984, 2003.

- [4] W.G. Mook. Abundance and fractionation of stable isotopes. In W.G. Mook, editor, *Environmental Isotopes in the Hydrological Cycle. Principles and Applications*, volume 1, chapter 3, pages 31–48. UNESCO Publishing, Paris, 2000.
- [5] F.N. von Hippel. Plutonium and reprocessing of spent nuclear fuel. *Science*, 293(5539):2397–2398, 2001.
- [6] J.P. McBride, R.E. Moore, J.P. Witherspoon, and R.E. Blanco. Radiological impact of airborne effluents of coal and nuclear plants. *Science*, 202(4372):1045–1050, 1978.
- [7] M. Bruenglinghaus. *European Nuclear Society*, 2012 (last accessed June 28, 2012). <http://www.euronuclear.org>.
- [8] ANS. *American Nuclear Society*, 2012 (last accessed June 28, 2012). <http://www.ans.org>.
- [9] R.A. de Vries, M. de Bruin, J.J. Marx, and A. Van de Wiel. Radioisotopic labels for blood cell survival studies: a review. *Nuclear Medicine and Biology*, 20(7):809–817, 1993.
- [10] J.E. Van Eyk and M.J. Dunn. *Clinical Proteomics: From Diagnosis to Therapy*. Wiley-VCH Verlag, Weinheim, 2008.
- [11] P. Ciais, P.P. Tans, M. Trolier, J.W.C. White, and R.J. Francey. A large northern hemisphere terrestrial CO₂ sink indicated by the ¹³C/¹²C ratio of atmospheric CO₂. *Science*, 269(5227):1098–1102, 1995.
- [12] P.A. de Groot. Carbon. In P.A. de Groot, editor, *Handbook of Stable Isotope Analytical Techniques*, volume 2, chapter 4, pages 229–329. Elsevier, Amsterdam, first edition, 2009.
- [13] J. Bigeleisen. Isotopes. *Annual Review of Physical Chemistry*, 3:39–56, 1952.
- [14] O. Bilous and F. Doneddu. Process control of a gaseous diffusion cascade for isotopic separation of uranium. *Chemical Engineering Science*, 41(6):1403–1415, 1986.
- [15] J. Bigeleisen. Chemistry of isotopes. *Science*, 147(3657):463–471, 1965.
- [16] W.J. Thomas and S.B. Watkins. The separation of common gases by thermal diffusion. *Chemical Engineering Science*, 5(1):34–49, 1956.
- [17] OECD/Nuclear Energy Agency. *Beneficial Uses and Production of Isotopes*. OECD Publishing, Paris, 2005.

- [18] H.C. Urey. The thermodynamic properties of isotopic substances. *Journal of the Chemical Society*, pages 562–581, 1947.
- [19] J. Bigeleisen and M.G. Mayer. Calculation of equilibrium constants for isotopic exchange reactions. *The Journal of Chemical Physics*, 15(5):261–267, 1947.
- [20] A. de la Garza. Multicomponent isotope separation in cascades. *Chemical Engineering Science*, 17(9):709–710, 1962.
- [21] P.A. de Groot. Isotope separation methods. In P.A. de Groot, editor, *Handbook of Stable Isotope Analytical Techniques*, volume 2, chapter 20, pages 1025–1032. Elsevier, Amsterdam, first edition, 2009.
- [22] W.A. Van Hook. Isotope separation. In A. Vértés, S. Nagy, and Z. Klencsár, editors, *Handbook of Nuclear Chemistry*, volume 5, chapter 5, pages 177–211. Kluwer Academic Publishers, Dordrecht, 2003.
- [23] K.P. Cohen. Manhattan Project Technical Section, Division III. In G.M. Murphy, editor, *The Theory of Isotope Separation as Applied to the Large-Scale Production of U^{235}* , volume 1B of *National Nuclear Energy Series*. McGraw-Hill, New York, first edition, 1951.
- [24] H. London. *Separation of Isotopes*. George Newnes Limited, London, 1961.
- [25] B.B. McInteer. Isotope separation by distillation: Design of a carbon-13 plant. *Separation Science and Technology*, 15(3):491–508, 1980.
- [26] B.M. Andreev, E.P. Magomedbekov, A.A. Raitman, M.B. Pozenkevich, Yu.A. Sakharovsky, and A.V. Khoroshilov. *Separation of Isotopes of Biogenic Elements in Two-phase Systems*. Elsevier, Amsterdam, 2007.
- [27] D.C. Dumitrache, B. De Schutter, A. Huesman, and E. Dulf. Modeling, analysis, and simulation of a cryogenic distillation process for ^{13}C isotope separation. *Journal of Process Control*, 22(4):798–808, 2012.
- [28] M.W. Zemansky and R.H. Dittman. *Heat and Thermodynamics*. McGraw-Hill, New York, seventh edition, 1997.
- [29] E.L. Cussler. *Diffusion. Mass Transfer in Fluid Systems*. Cambridge University Press, Cambridge, third edition, 2009.

- [30] C.J. King. *Separation Processes*. McGraw-Hill, New York, second edition, 1980.
- [31] J. Benitez. *Principles and Modern Applications of Mass Transfer Operations*. John Wiley & Sons, Inc., Hoboken, second edition, 2009.
- [32] I.J. Halvorsen and S. Skogestad. Theory of Distillation. In I.D. Wilson, E.R. Adlard, M. Cooke, and C.F. Poole, editors, *Encyclopedia of Separation Science*, pages 1117–1134. Academic Press, San Diego, 2000.
- [33] S. Skogestad. Dynamics and control of distillation columns: A tutorial introduction. *Chemical Engineering Research and Design*, 75(6):539–562, 1997.
- [34] S. Skogestad and M. Morari. Design of resilient processing plants-IX. Effect of model uncertainty on dynamic resilience. *Chemical Engineering Science*, 42(7):1765–1780, 1987.
- [35] S. Skogestad and M. Morari. LV-Control of a high-purity distillation column. *Chemical Engineering Science*, 43(1):33–48, 1988.
- [36] E. Sørensen and S. Skogestad. Comparison of regular and inverted batch distillation. *Chemical Engineering Science*, 51(22):4949–4962, 1996.
- [37] H.-X. Li and C. Qi. Modeling of distributed parameter systems for applications - a synthesized review from time-space separation. *Journal of Process Control*, 20(8):891–901, 2010.
- [38] H.-X. Li and C. Qi. *Spatio-Temporal Modeling of Nonlinear Distributed Parameter Systems. A Time/Space Separation Based Approach*, volume 50 of *International Series on Intelligent Systems, Control, and Automation: Science and Engineering*. Springer, Dordrecht, 2011.
- [39] R. Curtain and K. Morris. Transfer functions of distributed parameter systems: A tutorial. *Automatica*, 45(5):1101–1116, 2009.
- [40] L. Debnath. *Nonlinear Partial Differential Equations for Scientists and Engineers*. Birkhäuser, Boston, second edition, 2005.
- [41] D.G. Duffy. *Transform Methods for Solving Partial Differential Equations*. Chapman & Hall/CRC, Boca Raton, second edition, 2000.
- [42] E.J. Townsend. *Functions of a Complex Variable*. Henry Holt and Company, New York, 1915.

- [43] W.R. LePage. *Complex Variables and the Laplace Transform for Engineers*. Dover Publications, New York, 1980.
- [44] D.G. Duffy. *Advanced Engineering Mathematics*. CRC Press, Boca Raton, 1998.
- [45] J.W. Brown and R.V. Churchill. *Complex Variables and Applications*. McGraw-Hill, Boston, eighth edition, 2009.
- [46] P.D. Lax and R.D. Richtmyer. Survey of the stability of linear finite difference equations. *Communications on Pure and Applied Mathematics*, 9:267–293, 1956.
- [47] T.J. Chung. *Computational Fluid Dynamics*. Cambridge University Press, Cambridge, second edition, 2010.
- [48] J.C. Strikwerda. *Finite Difference Schemes and Partial Differential Equations*. SIAM: Society for Industrial and Applied Mathematics, Philadelphia, second edition, 2004.
- [49] A. Rutherford. *Mathematical Modeling Techniques*. Dover Publications, Inc., Mineola, 1994.
- [50] A. Rutherford. *Mathematical Modeling: A Chemical Engineer’s Perspective*, volume 1 of *Process Systems Engineering*. Academic Press, San Diego, 1999.
- [51] D. Basmadjian. *The Art of Modeling in Science and Engineering*. Chapman&Hall/CRC, Boca Raton, 1999.
- [52] A.M. Law and W.D. Kelton. *Simulation Modeling and Analysis*. McGraw-Hill Series on Industrial Engineering and Management Science. McGraw-Hill, Boston, third edition, 2000.
- [53] M. Mangold, S. Motz, and E.D. Gilles. A network theory for the structured modelling of chemical processes. *Chemical Engineering Science*, 57(19):4099–4116, 2002.
- [54] R.F. Taylor. Chemical engineering problems of radioactive waste fixation by vitrification. *Chemical Engineering Science*, 40(4):541–569, 1985.
- [55] G. Jancso and W.A. Van Hook. Condensed phase isotope effects (especially vapor pressure isotope effects). *Chemical Reviews*, 74(6):689–750, 1974.
- [56] J.A. Mandler. Modelling for control analysis and design in complex industrial separation and liquefaction processes. *Journal of Process Control*, 10(2-3):167–175, 2000.

- [57] Air Liquide Group. *Physical properties of gases, safety, MSDS, enthalpy, material compatibility, gas liquid equilibrium, density, viscosity, flammability, transport properties*, 2012 (last accessed June 14, 2012). <http://encyclopedia.airliquide.com>.
- [58] K.J. Åström and B. Wittenmark. *Computer-Controlled Systems: Theory and Design*. Prentice Hall Information and System Sciences Series. Prentice Hall, Upper Sadle River, third edition, 1997.
- [59] K. Ogata. *Modern Control Engineering*. Prentice Hall, Upper Sadle River, third edition, 1997.
- [60] S.J. Farlow. *Partial Differential Equations for Scientists and Engineers*. Dover Publications, Mineola, 1993.
- [61] H. Dwyer. The Laplace transform: Motivating the definition. *CODEE Journal*, 2011 (last accessed July 2, 2012). <http://www.codee.org/ref/CJ11-0116>.
- [62] K. Cohen. Packed fractionation columns and the concentration of isotopes. *The Journal of Chemical Physics*, 8:588–597, 1940.
- [63] M. Benedict, T.H. Pigford, and H.W. Levi. *Nuclear Chemical Engineering*. Series in Nuclear Engineering. McGraw-Hill Book Company, New York, second edition, 1981.
- [64] S. Howison. *Practical Applied Mathematics: Modelling, Analysis, Approximation*. Cambridge University Press, Cambridge, 2005.
- [65] J. Stewart. *Calculus*. Brooks/Cole Publishing Company, Pacific Grove, fourth edition, 1999.
- [66] J. Stewart. *Calculus. Early Transcendentals*. Thomson Brooks/Cole Publishing Company, Belmont, sixth edition, 2008.
- [67] B.S. Grewal. *Higher Engineering Mathematics*. Khanna Publishers, New Delhi, thirty-sixth edition, 2001.
- [68] L. Debnath and D. Bhatta. *Integral Transforms and Their Applications*. Chapman & Hall/CRC, Boca Raton, second edition, 2007.
- [69] T.J. I’A. Bromwich. Normal coordinates in dynamical systems. *Proceedings of the London Mathematical Society*, s2-15(1):401–448, 1917.

- [70] A. Erdelyi, W. Magnus, F. Oberhettinger, and F.C. Tricomi, editors. *Tables of Integral Transforms*, volume 1. McGraw-Hill Book Company, New York, 1954.
- [71] A. Erdelyi, W. Magnus, F. Oberhettinger, and F.C. Tricomi, editors. *Tables of Integral Transforms*, volume 2. McGraw-Hill Book Company, New York, 1954.
- [72] W.O. Pennell. A generalization of Heaviside's Expansion Theorem. *Bell System Technical Journal*, 8(i3):482–492, 1929.
- [73] J. Bird. *Higher Engineering Mathematics*. Elsevier, Amsterdam, fifth edition, 2006.
- [74] MathWorks. *MathWorks - MATLAB and Simulink for Technical Computing*, 2012 (last accessed June 7, 2012). <http://www.mathworks.com/>.
- [75] R.P. Brent. *Algorithms for Minimization Without Derivatives*. Prentice Hall, Englewood Cliffs, 1973.
- [76] M.J. Modest. *Radiative Heat Transfer*. Academic Press, Amsterdam, Second edition, 2003.
- [77] C.K. Krishnaprakas, K. Badari Narayana, and P. Dutta. Heat transfer correlations for multilayer insulation systems. *Cryogenics*, 40(7):431–435, 2000.
- [78] DW Designs. *Emissivity Materials*, 2012 (last accessed June 14, 2012). <http://www.infrared-thermography.com/material.htm>.